⌘ *Author's Choice*

THE JOURNAL OF BIOLOGICAL CHEMISTRY VOL. 288, NO. 1, pp. 255–263, January 4, 2013

Increase in Serum Ca^{2+}/Mg^{2+} Ratio Promotes Proliferation of Prostate Cancer Cells by Activating TRPM7 Channels*[S]

Received for publication, June 21, 2012, and in revised form, November 19, 2012 Published, JBC Papers in Press, November 20, 2012, DOI 10.1074/jbc.M112.393918

Yuyang Sun[‡], Senthil Selvaraj[‡], Archana Varma[§], Susan Derry[§], Abe E. Sahmoun[§], and Brij B. Singh[‡1]

From the Departments of [‡]Biochemistry and Molecular Biology and [§]Internal Medicine, School of Medicine and Health Sciences, University of North Dakota, Grand Forks, North Dakota 58201

Background: Mg^{2+} concentration regulates MagNuM channels; however, their role in prostate cancer is not known.
Results: TRPM7 functions as an endogenous MagNuM channel, which facilitates Ca^{2+} entry at low Mg^{2+} levels and promotes cell proliferation.
Conclusion: Alteration in Ca^{2+}/Mg^{2+} ratio could lead to prostate cancer.
Significance: Learning how extra/intracellular Ca^{2+}/Mg^{2+} ratio is regulated is crucial for understanding and/or diagnosis of prostate cancer.

TRPM7 is a novel magnesium-nucleotide-regulated metal current (MagNuM) channel that is regulated by serum Mg^{2+} concentrations. Changes in Mg^{2+} concentration have been shown to alter cell proliferation in various cells; however, the mechanism and the ion channel(s) involved have not yet been identified. Here we demonstrate that TRPM7 is expressed in control and prostate cancer cells. Supplementation of intracellular Mg-ATP or addition of external 2-aminoethoxydiphenyl borate inhibited MagNuM currents. Furthermore, silencing of TRPM7 inhibited whereas overexpression of TRPM7 increased endogenous MagNuM currents, suggesting that these currents are dependent on TRPM7. Importantly, although an increase in the serum Ca^{2+}/Mg^{2+} ratio facilitated Ca^{2+} influx in both control and prostate cancer cells, a significantly higher Ca^{2+} influx was observed in prostate cancer cells. TRPM7 expression was also increased in cancer cells, but its expression was not dependent on the Ca^{2+}/Mg^{2+} ratio *per se*. Additionally, an increase in the extracellular Ca^{2+}/Mg^{2+} ratio led to a significant increase in cell proliferation of prostate cancer cells when compared with control cells. Consistent with these results, age-matched prostate cancer patients also showed a subsequent increase in the Ca^{2+}/Mg^{2+} ratio and TRPM7 expression. Altogether, we provide evidence that the TRPM7 channel has an important role in prostate cancer and have identified that the Ca^{2+}/Mg^{2+} ratio could be essential for the initiation/progression of prostate cancer.

Ca^{2+} signaling is essential for regulating physiological functions such as cell proliferation and differentiation (1–3). Prostate cancer (PCa)[2] is the second most lethal tumor among men, and Ca^{2+} has been shown to be essential for increased cell proliferation in prostate cells (4–6). However, the ion channel(s) involved in increased Ca^{2+} entry that can lead to an increase in cell proliferation is not fully understood. Additionally, the mechanism that leads to alterations in Ca^{2+} handling in PCa is still poorly defined. Understanding the factors that drive PCa toward increased cell proliferation is crucial for the development of new therapies that can prevent and/or inhibit initiation and/or progression of PCa. Importantly, early stage PCa depends on androgens that are needed for its growth, and because these androgens also regulate Ca^{2+} entry, it can be anticipated that abnormal Ca^{2+} signaling may be an essential step toward increased cell proliferation and in the development of PCa (7–9). In addition, besides Ca^{2+}, other ions such as Mg^{2+} also play a critical role in cell proliferation (10, 11); however, the mechanism and the importance of the tight balance between these ions especially in PCa is still unclear.

Mg^{2+} is the second most common cation in intracellular fluids. Appropriate Mg^{2+} levels have been shown to be involved in physiological functions such as nucleic acid metabolism, protein synthesis, and energy production (12, 13). Interestingly, recently it has also been proposed that Mg^{2+} could also initiate cell proliferation upon mitogenic stimulus because cells are able to increase their intracellular Mg^{2+} content by activating Mg^{2+} influx, which is needed for initiation of protein synthesis (14, 15). Therefore, influx of both extracellular Ca^{2+} and Mg^{2+} needs to be tightly maintained for proper intracellular ion homeostasis. Furthermore, alterations in this homeostasis will likely increase cell proliferation and can lead to cancer. An increase in cytosolic Ca^{2+} has also been shown to regulate apoptosis (16, 17). Thus, a tight balance between Ca^{2+} and Mg^{2+} ions is needed. Additionally, loss of this balance can alter the normal functioning of the cell and promote cell proliferation, thereby inducing a more cancerous phenotype. Thus, identification of the ion channel that can regulate this tight balance is important to understand how cells adapt a more cancerous phenotype.

Melastatin-like transient receptor potential (TRPM) subfamilies are a diverse group of voltage-independent Ca^{2+}-permeable cation channels that are expressed in mammalian cells

* This work was supported, in whole or in part, by National Institutes of Health Grants RO1 DE017102 and 5P20RR017699 (to B. B. S.).
⌘ *Author's Choice*—Final version full access.
[S] This article contains supplemental Fig. S1.
[1] To whom correspondence should be addressed. Tel.: 701-777-0834; Fax: 701-777-2382; E-mail: brij.singh@med.und.edu.
[2] The abbreviations used are: PCa, prostrate cancer; MagNuM, magnesium-nucleotide-regulated metal current; 2APB, 2-aminoethoxydiphenyl borate; TRPM, melastatin-like transient receptor potential; MTT, 3-(4,5-dimethylthiazol-2-yl)-2,5-diphenyltetrazolium bromide; pF, picofarad; IV, current-voltage; NMDG, *N*-methyl-D-glucamine.

(18–21). Two of these members, TRPM6 and TRPM7, are unique because they possess an enzyme domain in their C termini and have been shown to be regulated by intracellular levels of Mg^{2+}-complexed nucleotides (22). Interestingly, TRPM6/7 have been shown to be spontaneously activated that will conduct Ca^{2+} and Mg^{2+} at negative membrane potentials, and the current is strongly activated when Mg-ATP falls below 1 mM (designated MagNuM for magnesium-nucleotide-regulated metal current) (20). TRPM6/7 channels are widely expressed ion channels and recently have been shown to be associated with cell proliferation and survival (22); however, their function and expression in prostate cancer cells is not known. Mutations in the TRPM6/7 gene have also been shown in patients suffering from a hereditary form of hypomagnesaemia caused by impaired Mg^{2+} reabsorption (23), suggesting an unequivocal role of these channels in Mg^{2+} homeostasis. Consistent with this, TRPM7-deficient DT40 cells showed decreased cell proliferation that was rescued by adding extracellular Ca^{2+} or Mg^{2+} (24). Nevertheless, despite considerable progress in the understanding of MagNuM currents, the molecular nature of the channels involved in proliferation of prostate cancer cells, which can contribute to the development of PCa, remains unknown.

The data presented here indicate that TRPM7 functions as an endogenous MagNuM channel in prostate cancer cells and that a decrease in extracellular Mg^{2+} concentration potentiates MagNuM currents specifically in prostate cancer cells. Interestingly, in prostate cancer cells, TRPM7 also potentiated Ca^{2+} currents, and an increase in extracellular Ca^{2+} or a decrease in extracellular Mg^{2+} further increased Ca^{2+} influx. Finally, this increase in Ca^{2+} influx due to a higher Ca^{2+}/Mg^{2+} ratio was critical to promote cell proliferation without altering the expression levels of TRPM7. Consistent with these results, the serum Ca^{2+}/Mg^{2+} ratio was also increased in prostate cancer patients, indicating that the Ca^{2+}/Mg^{2+} ratio is perhaps critical for cell proliferation in prostate cancer cells.

EXPERIMENTAL PROCEDURES

Cell Culture Reagents and Silencing of TRPM7—Control prostate cell line RWPE (CRL 11609) and prostate cancer cell lines DU145 (HTB-81) and PC3 (CRL1435) were obtained from the American Type Culture Collection (Manassas, VA). Cells were cultured in their respective medium along with various supplements as suggested by ATCC. Cells were maintained at 37 °C with 95% humidified air and 5% CO_2 and passaged as needed. Culture medium was changed twice weekly, and cells were maintained in complete medium until reaching 90% confluence, then trypsinized, centrifuged, and resuspended in the same medium as described before (25). For various ion contents, cells were resuspended in DMEM devoid of calcium and magnesium ions, and both calcium and magnesium ions were supplemented as needed. For RNAi experiments, shRNA that targets the coding sequence of human TRPM7 was obtained from Origene Technologies, and a FITC-conjugated non-targeting shRNA was used as a control. Cells were transfected with individual shRNA (50 nM) using Lipofectamine 2000 in Opti-MEM according to the supplier's instructions (Invitrogen) and assayed after 48 h. For overexpression, HA-TRPM7 was used, and 5 μg of plasmid DNA was transformed using Lipofectamine 2000 in Opti-MEM according to the supplier's instructions and assayed after 24 h. Antibodies that were used in this study are described in the figures. All other reagents used were of molecular biology grade obtained from Sigma unless mentioned otherwise.

Cell Viability Assays—Cells were seeded on 96-well plates at a density of 0.5×10^5 cells/well. The cultures were grown for 24 h followed by addition of fresh medium prior to the experiment. Cell viability was measured by using the Vibrant MTT cell proliferation assay kit (Molecular Probes, Eugene, OR). 30 μl of MTT reagent (0.5 mg/ml MTT in PBS containing 10 μM Hepes) was added to each well and incubated in a CO_2 incubator for 2 h. The medium was aspirated from each well, and the culture plate was dried at 37 °C for 1 h. The resulting formazan dye was extracted with 100 μl of 0.04 N HCl in isopropanol, and the absorbance was measured in a microplate reader (Molecular Devices, Sunnyvale, CA) at 570 and 630 nm. Cell viability was expressed as a percentage of the control culture. Trypan blue staining was also used to study cell proliferation and to differentiate between live and dead cells. Cells (5×10^6 cells/well) were grown in 24-well plates under different conditions for 48 h, trypsinized, stained using an equal volume of trypan blue, and counted using a light microscope.

Electrophysiology—For patch clamp experiments, coverslips with cells were transferred to the recording chamber and perfused with an external Ringer's solution of the following composition: 145 mM NaCl, 5 mM CsCl, 1 mM $MgCl_2$, 1 mM $CaCl_2$, 10 mM Hepes, 10 mM glucose, pH 7.3 (NaOH). Hepes was replaced by Mes for the solutions at pH ≤6.0. Whole cell currents were recorded using an Axopatch 200B (Axon Instruments, Inc.). The patch pipette had resistances between 3 and 5 megaohms after filling with the standard intracellular solution of the following composition: 150 mM cesium methane sulfonate, 8 mM NaCl, 10 mM Hepes, 10 mM EGTA, pH 7.2 (CsOH). With a holding potential of 0 mV, voltage ramps ranging from −100 to +100 mV and of 100-ms duration were delivered at 2-s intervals after whole cell configuration was formed. Currents were recorded at 2 kHz and digitized at 5–8 kHz. pClamp 10.1 software was used for data acquisition and analysis. Basal leak was subtracted from the final currents, and average currents are shown. All experiments were carried out at room temperature.

Membrane Preparations and Western Blot Analyses—Cells were harvested and stored at −80 °C. Crude lysates were prepared from RWPE and DU145 cells as described previously (25). Protein concentrations were determined using the Bradford reagent (Bio-Rad), and 25–50 μg of proteins was resolved on 3–8% SDS-Tris acetate gels, transferred to PVDF membranes, and probed with respective antibodies. A 1:500 dilution for TRPM7 (Epitomics) and a 1:1000 dilution for actin (Santa Cruz Biotechnology) antibodies were used to probe respective proteins. Peroxidase-conjugated respective secondary antibodies were used to label the proteins. Proteins on the membrane were detected using ECL reagent (Pierce) and analyzed using a Lumi-Imager (Roche Applied Science) as described (25–28).

Confocal Microscopy—For immunofluorescence, cells were grown overnight on coverslips, washed twice with PBS, and fixed for 30 min using 3% paraformaldehyde. Cells were then

permeabilized using cold methanol and blocked for 20 min using 5% donkey serum. For TRPM7 staining, cells were treated with anti-TRPM7 antibody at a 1:100 dilution for 1 h. Cells were washed (three times with PBS, 0.5% BSA) and labeled with rhodamine-linked anti-rabbit secondary antibody (1:100 dilution) (24, 30). Confocal images were collected using an MRC 1024-krypton/argon laser-scanning confocal microscope equipped with a Zeiss LSM 510 Meta photomicroscope.

Quantitative RT-PCR—TRPM7 mRNA expression was assessed with real time RT-PCR using commercially available primers (Origene Technologies). cDNA was transcribed from 1 μg of total RNA with iScript cDNA (Bio-Rad). An equal amount of cDNA template was added to iQ SYBR Green Supermix together with appropriate primers at 0.2 μM each. Quantitative PCR was performed using an iCycler iQ real time detection system following the specifications of the manufacturer. The relative level of mRNA was interpolated from each sample. GAPDH was used for normalization of the transcripts. Specificity of PCR product formation was confirmed by monitoring melting peaks.

Study Design and Statistical Analyses—A retrospective analysis of medical charts of patients that were diagnosed with prostate cancer between 2000 and 2011 was performed. Cases were identified from the cancer registry at Altru hospital, North Dakota. Controls from the same hospital that were negative for prostate-specific antigen or prostate biopsies were also used. The study was approved by the Institutional Review Boards of the hospital and the University of North Dakota. Data on age, histology, prostate-specific antigen were abstracted using electronic records. The inclusion criterion for cases was men with histologically confirmed prostate cancer as a primary site with cancer diagnosed between 2000 and 2011. The exclusion criteria included diagnosis of any cancer other than primary prostate cancer. The inclusion criterion for controls was men who had an annual physical exam between 2000 and 2010 at the same hospital as cases without cancer. χ^2 or Fisher's exact tests were used to analyze the differences between groups for categorical variables, and *t* tests were used for continuous variables. All *p* values are two-sided, and statistical significance was defined as *p* values <0.05. Analyses were performed using SAS software V9.1.3 (SAS Institute, Cary, NC).

RESULTS

Functional Characterization of MagNuM Channel in Prostate Cells—In prostate cells, Mg^{2+} ion is not only crucial for DNA regulation but is also essential for regulating other cellular functions such as cell proliferation. However, the identity of the channel that regulates intracellular Mg^{2+} levels in prostate cells is not known. We show here that both control prostate cells (RWPE) and prostate cancer cells (DU145 and PC3) showed inward and outward rectifying currents that were prompted using a voltage ramp protocol only in conditions in which intracellular Mg^{2+} was decreased. Using NaCl-based extracellular solutions containing physiological concentrations of $CaCl_2$ and $MgCl_2$, both control and prostate cancer cells showed a large outward rectifying current that reversed close to 0 mV. The current properties were consistent with previous recordings observed in different cells that have been shown to be linked with TRPM7 channels (20, 29–31). In control prostate cells, the outward rectifying currents appeared gradually and reached a plateau within 400 s after initiation (by eliminating intracellular Mg^{2+}) of the whole cell recording. Interestingly, under these conditions, the amplitude of the current observed was not significantly different in control or prostate cancer cells (at -100 mV, 1.42 ± 0.55 pA/pF was observed in control cells, whereas 0.93 ± 0.16 pA/pF was observed in prostate cancer cells) (Fig. 1, *A* and *C*; IV curves are shown in Fig. 1, *B* and *D*). The average current density recorded at both positive and negative potentials is presented in Fig. 1*G*. Similarly, the outward current was also not significantly different in control and cancer cells (at $+100$ mV, the current density was 17.0 pA/pF for control, whereas 23.9 pA/pF was observed in DU145 and 16.3 pA/pF was observed in PC3 prostate cancer cells) (Fig. 1, *E*–*G*).

To confirm that the channels are indeed mediated by TRPM7, channel properties were evaluated at various pH values, which again showed that lowering the pH increased the maximum current intensity (Fig. 1*H*). Furthermore, large inward currents were observed upon removal of all extracellular divalent cations (Fig. 1, *I* and *J*), consistent with previous studies (30). In addition, outward currents, but not inward currents, were reduced when NMDG was added in the extracellular solution (Fig. 1*K*), suggesting that the outward currents are only partially dependent on Na^+ efflux. Finally, current-voltage relations were also evaluated in the presence of varying extracellular Ca^{2+} and Mg^{2+} solutions, which showed a preference toward Mg^{2+} entry over Ca^{2+}. However, in the absence of Mg^{2+}, the channels were able to conduct Ca^{2+} currents (Fig. 1*L*).

To investigate whether we can separate the MagNuM currents on the basis of their pharmacological properties, we studied the effects of 2APB on these cells. It has been shown previously that TRPM6 currents are potentiated by the addition of 2APB, whereas TRPM7 currents are significantly inhibited by addition of similar concentrations of 2APB (32, 33). Extracellular addition of 500 μM 2APB dramatically decreased MagNuM current amplitude in control cells (Fig. 2, *A* and *C*), indicating that the channel is mainly mediated by TRPM7. Consistent with these results, prostate cancer cells also showed a significant decrease in the channel conductance, and addition of 2APB also decreased MagNuM currents (Fig. 2, *B* and *C*). Importantly, removal of 2APB from the extracellular solutions further potentiated the currents (Fig. 2*D*), suggesting that TRPM7 rather than TRPM6 underlies this current. Surprisingly, unlike control cells, 2APB did not completely inhibit the MagNuM currents observed in cancer cells, suggesting that other channels can also play a role in these cells. Finally, to confirm that the channel properties are indeed dependent on TRPM7, we silenced TRPM7 expression using siRNA. As indicated in Fig. 2*E*, control cells transfected with TRPM7siRNA, but not control siRNA, showed a significant decrease in TRPM7 protein levels (Fig. 2*E*). Furthermore, both outward and inward currents were significantly decreased in both control and prostate cancer cells that expressed TRPM7 siRNA (Fig. 2, *F* and *G*). Importantly, the channel properties were not changed, suggesting that TRPM7 is the major MagNuM channel in these cells. In addition, we also overexpressed TRPM7 in

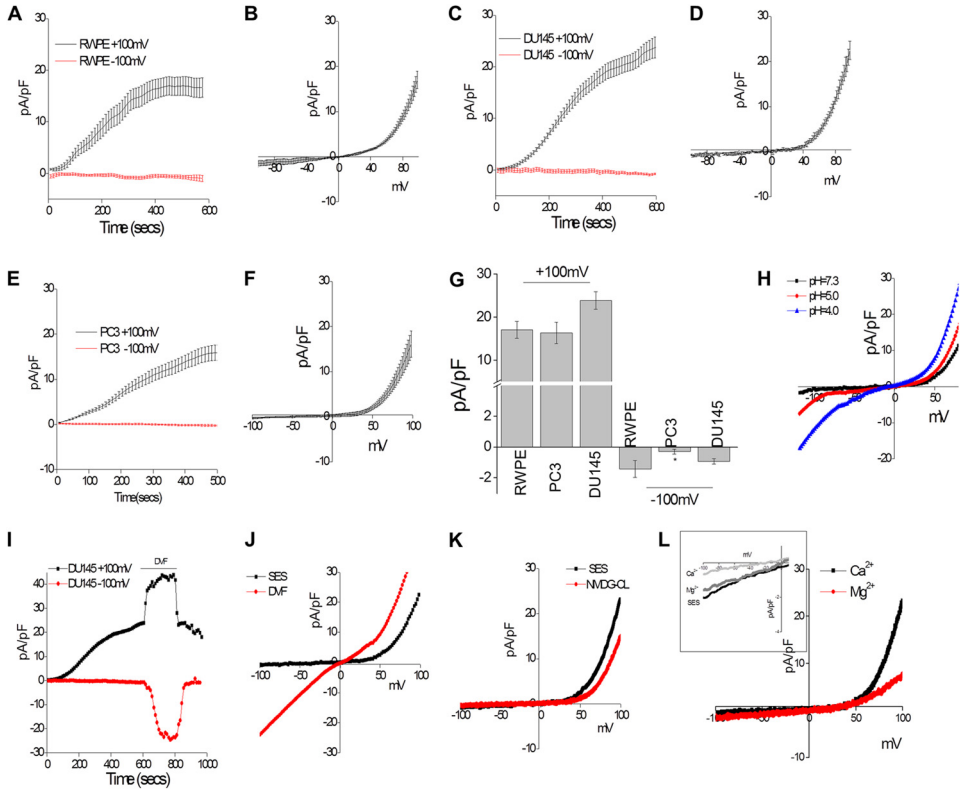

FIGURE 1. **Characterization of intracellular Mg^{2+}-dependent inward and outward rectifying currents in control and prostate cancer cells.** *A*, representative traces showing changes of whole cell currents in conditions of 1.2 mM Mg^{2+} and 1.5 mM Ca^{2+} external solution from normal prostate cells (RWPE) that were activated by the depletion of intracellular Mg^{2+}. Outward currents (*top* curve) were measured at +100 mV; inward currents (*bottom* curve; *red*) were measured at −100 mV. Average IV curves (developed from maximum currents) under this condition are shown in *B*. *C* and *E*, changes of whole cell currents under similar conditions from prostate cancer cells (DU145 and PC3) are shown. Outward currents were again measured at +100 mV; inward currents were measured at −100 mV (*bottom* line; *red*). IV curves (developed from maximum currents) of these cells under this condition are shown in *D* and *F*. *G*, average (8–10 recordings) current intensity at +100 and −100 mV under these conditions is shown. *H*, representative IV curves of prostate cancer cells (DU145) under conditions of pH 7.3, pH 5.0, and pH 4.0. Time courses of membrane current recorded on prostate cancer cells (DU145) are shown in *I*. Removal of bath Ca^{2+} and Mg^{2+} (divalent ion-free (*DVF*)) induced a remarkable increase of inward and outward currents. IV curves of corresponding time points are shown in *J*. *K*, representative IV curves of prostate cancer cells (DU145) under conditions of standard external solution (*SES*) (1.2 mM Mg^{2+}, 1.5 mM Ca^{2+}, and 145 mM Na^{+}) and NMDG-Cl (Na^{+} replaced with NMDG in the external solution). *L*, representative IV curves of prostate cancer cells (DU145) under conditions of 3 mM Ca^{2+} and 150 mM NMDG-Cl external solution or 3 mM Mg^{2+} and 150 mM NMDG-Cl external solution. The *inset* shows a magnified view of the reverse potential under different conditions. *Error bars* represent ±S.E.

DU145 cells, which showed an increase in the outward and inward currents (Fig. 2*G*).

Mg-ATP Levels Inhibit MagNuM Currents, Which Are Mediated by TRPM7, in Prostate Cells—To further characterize these currents, we also used Mg-ATP because these channels have been shown to be activated by reduction in free intracellular Mg^{2+} or Mg-ATP concentrations *per se*. Under similar extracellular conditions, both inward and outward currents were decreased with intracellular application of 2 mM Mg-ATP (Fig. 3, *A–E*). Addition of intracellular Mg-ATP completely blocked MagNuM currents in normal prostate cells (Fig. 3, *A* and *B*; average density is shown in Fig. 3*E*). Surprisingly, similar concentrations of Mg-ATP did not completely inhibit the MagNuM currents in prostate cancer cells; however, the overall current density was still decreased (Fig. 3, *C–E*) when compared with cells without Mg-ATP (Fig. 1, *C* and *D*), suggesting that perhaps a higher concentration of Mg-ATP is needed to completely block MagNuM channels in cancer cells. Finally, TRPM7 localization was also observed using confocal microscopy, which showed expression of TRPM7 at the plasma membrane in both cell types (Fig. 3*F*). Interestingly, a higher TRPM7 staining in the plasma membrane was observed in DU145 cells, further indicating that the differences in the properties could just be due to their variable expression patterns. Overall, the data presented in Figs. 1–3 strongly indicate that the currents observed here are similar to those shown with TRPM7 (30, 31) for which under physiological concentrations a small inward flux of divalent cations and a large outward flux of monovalent cations were observed.

Increase in Ca^{2+}/Mg^{2+} Ratio Facilitates Ca^{2+} Entry via the MagNuM Currents in Prostate Cancer Cells—We further investigated the importance of the Ca^{2+}/Mg^{2+} ratio in control and prostate cancer cells. An increase in the Ca^{2+}/Mg^{2+} ratio to 3.0 did not significantly increase the MagNuM currents in normal prostate cells (−1.47 ± 0.29 pA/pF at −100 mV and +21.20 ± 1.82 pA/pF at +100 mV) (Fig. 4, *A* and *B*; the average data are shown in Fig. 4*E*). In contrast, a significant increase in the MagNuM currents was observed in prostate cancer cells when the Ca^{2+} to Mg^{2+} ratio was increased to 3.0 (−1.51 ± 0.42 pA/pF at −100 mV and +35.10 ± 2.68 pA/pF at +100 mV) (Fig. 4, *C–E*). Importantly, no change in the IV properties of the channel was observed, suggesting that an increase in the Ca^{2+}/Mg^{2+} ratio affects Ca^{2+} permeability more in cancer cells as compared with control prostate cells. Interestingly, with a further increase

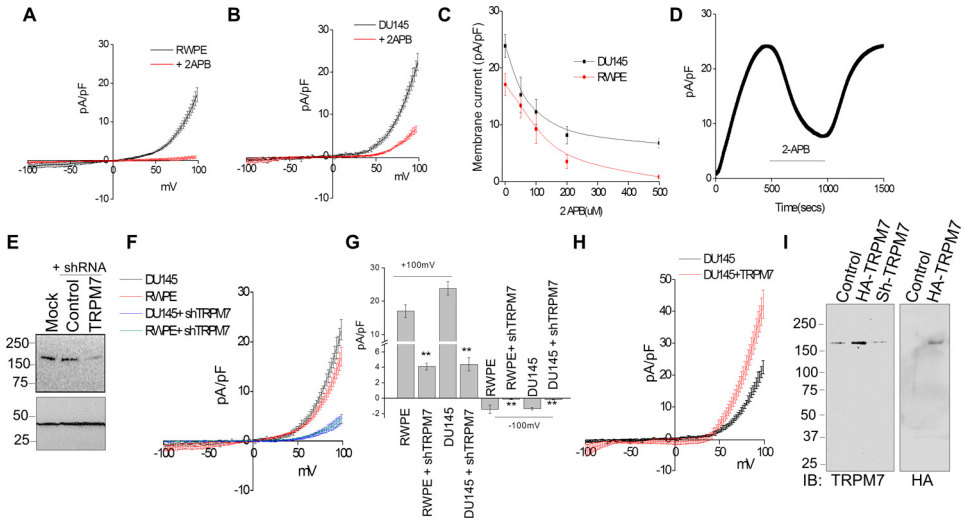

FIGURE 2. **Decrease in intracellular Mg^{2+} led to inward and outward rectifying currents that were dependent on TRPM7.** Bath application of 500 μM 2APB inhibited MagNuM current in RWPE and cancer cells, and average IV curves in control (*A*) and cancer cells (*B*) are shown. A dose-dependent inhibition of MagNuM currents by 2APB in RWPE and DU145 cells is shown in *C*. *D* represents outward currents in DU145 cells. Once the currents reached their peak, 500 μM 2APB was applied to the bath followed by recovery of the current by washing out 2APB. *E*, representative blots indicating DU145 cells expressing shRNA targeting TRPM7 or control non-targeting shRNA. *Mock* represents similar conditions without any shRNA plasmid. Cell lysates from DU145 cells were resolved on NuPAGE 3–8% Tris acetate gels and analyzed by Western blotting using TRPM7 antibodies (Epitomics). β-Actin was used as a loading control. Respective IV curves of cells transfected with shRNA targeting TRPM7 in RWPE and DU145 cells are show in *F*. Average (6–10 recordings) current intensity under these conditions in RWPE and DU145 cells are shown in *G*. ** indicates values (mean ± S.E.) that are significantly different from control ($p < 0.01$). *H*, IV curves from control or TRPM7-overexpressing prostate cancer cells (DU145). *I*, full blots of DU145 cells (control) or cells either overexpressing TRPM7 (*HA-TRPM7*) or TRPM7 shRNA (*Sh-TRPM7*). Western blots were performed either using TRPM7 or HA antibodies. *IB*, immunoblot. *Error bars* represent ±S.E.

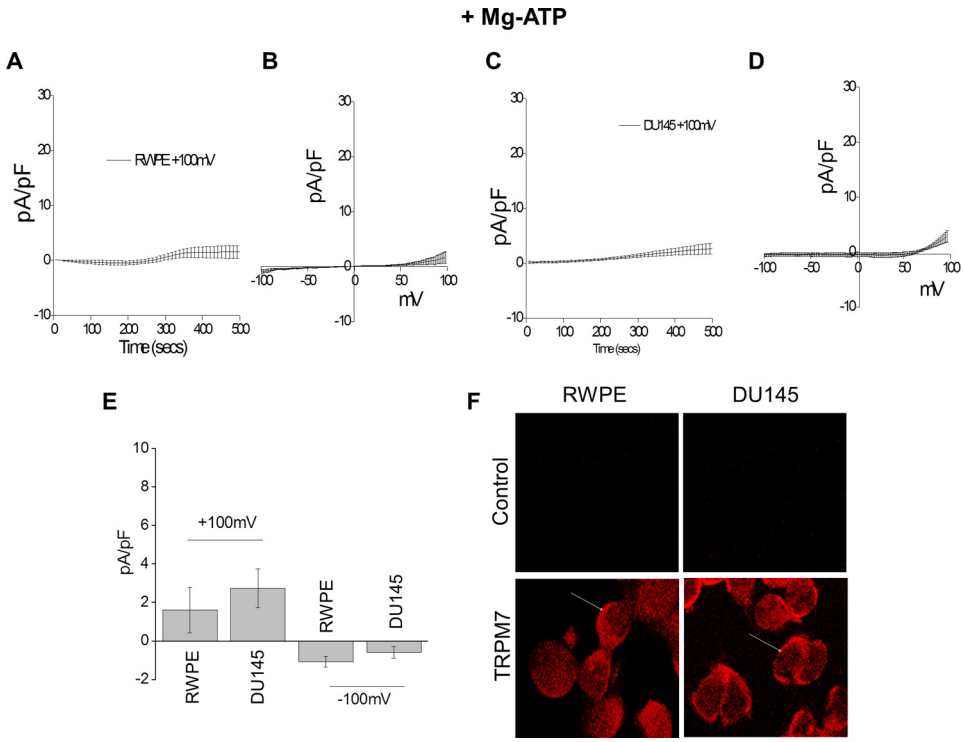

FIGURE 3. **Effect of intracellular Mg-ATP on prostate cells.** Individual representative traces showing inhibition of cation currents by intracellular application of 2 mM Mg-ATP on normal prostate cells (*A*) and prostate cancer cells (*C*) are shown. Respective IV curves (developed from maximum currents) under these conditions on normal prostate cells (*B*) and prostate cancer cells (*D*) are shown. *E*, average (6–10 recordings) current intensity at +100 and −100 mV under these conditions is shown. *F*, representative confocal images showing TRPM7 staining in control RWPE and DU145 cancer cells. Controls shown here are respective cells that did not receive the primary antibodies but were treated with the secondary antibodies. *Error bars* represent ±S.E.

in the Ca^{2+}/Mg^{2+} ratio to 5.0, the MagNuM currents in prostate cancer cells showed a greater increase in MagNuM channel activity (−3.87 ± 0.61 pA/pF at −100 mV and +42.67 ± 2.86 pA/pF at +100 mV) (Fig. 4, *H–J*, and supplemental Fig. S1, A and B), whereas the currents observed in normal prostate cells were not affected, and no further increase in MagNuM currents was observed (−2.11 ± 0.26 pA/pF at −100 mV and +28.03 ± 2.47 pA/pF at +100 mV) (Fig. 4, *F*, *G*, and *J*). These results

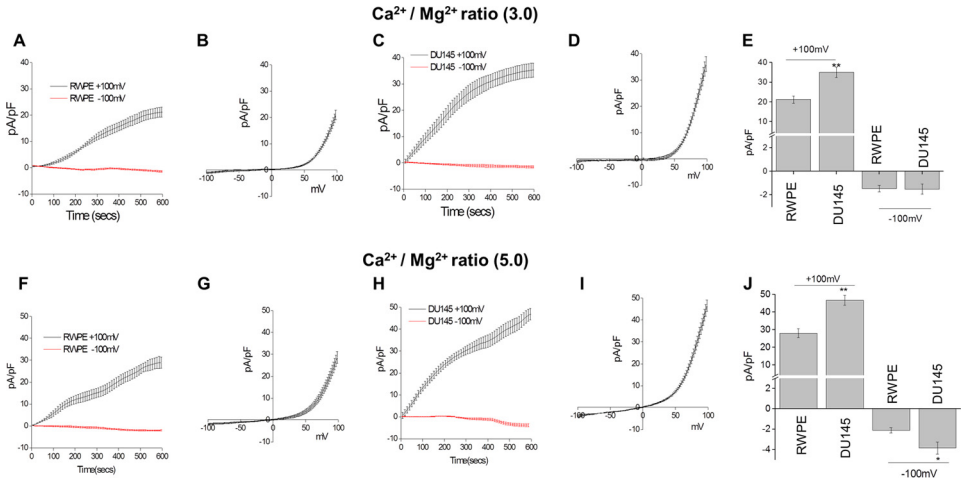

FIGURE 4. **MagNuM currents were increased when Ca^{2+}/Mg^{2+} ratio was increased in cancer cells.** *A*, representative traces showing changes of whole cell currents from normal prostate cells under conditions of a Ca^{2+}/Mg^{2+} ratio of 3.0 (or 3 mM Ca^{2+} and 0 mM Mg^{2+}) in external solution. *Top*, outward current measured at +100 mV; *bottom*, inward current measured at −100 mV. The IV curve under this condition is shown in *B*. *C*, representative traces showing changes of whole cell currents under similar conditions from prostate cancer cells. *Top*, outward current measured at +100 mV; *bottom*, inward current measured at −100 mV. The IV curve under this condition is shown in *D*. *E*, average (8–10 recordings) current intensity at +100 and −100 mV under these conditions. ** indicates values (mean ± S.E.) that are significantly different from control ($p < 0.01$). *F*, representative traces showing changes of whole cell currents from normal prostate cells under conditions of a Ca^{2+}/Mg^{2+} ratio of 5.0 (or 5 mM Ca^{2+} and 0 mM Mg^{2+}) in the external solution. *Top*, outward current measured at +100 mV; *bottom*, inward current measured at −100 mV. The IV curve under this condition is shown in *G*. *H*, changes of whole cell currents under similar conditions from prostate cancer cells. *Top*, outward current measured at +100 mV; *bottom*, inward current measured at −100 mV. The IV curve under this condition is shown in *I*. *J*, average (8–10 recordings) current intensity under these conditions. ** indicates values (mean ± S.E.) that are significantly different from control ($p < 0.01$). *Error bars* represent ±S.E.

suggest that the extracellular Ca^{2+}/Mg^{2+} ratio has a profound effect on MagNuM currents in prostate cancer cells but not in normal prostate cells, and in the absence of external Mg^{2+}, these cells will facilitate Ca^{2+} entry, which can promote cell proliferation.

Decreasing Extracellular Mg^{2+} and Increasing Ca^{2+}/Mg^{2+} Ratio Increase Cell Proliferation in Prostate Cancer Cells—The results shown above indicate that the MagNuM currents observed in prostate cells are mediated via TRPM7. In addition, our results also show that a decrease in intracellular Mg^{2+}/Mg-ATP levels activates these channels and facilitates Ca^{2+} entry when the Ca^{2+}/Mg^{2+} ratio is increased. Thus, we initially examined the expression of TRPM7 to determine whether its expression is also altered in different Ca^{2+}/Mg^{2+} conditions. As indicated in Fig. 5, *A* and *C*, TRPM7 was significantly increased in cancer cells when compared with control cells; however, no change in expression of TRPM7 was observed under various Ca^{2+}/Mg^{2+} conditions. To establish the relevance of the Ca^{2+}/Mg^{2+} ratio, we further assayed cell proliferation using varying Ca^{2+}/Mg^{2+} conditions. As shown in supplemental Fig. S1C, a significant increase in the rate of cell proliferation was observed in cancer cells that were incubated with increasing Ca^{2+} concentrations. We next investigated the consequences of the increased Ca^{2+} to Mg^{2+} ratio in cell growth and proliferation in these two different cell types. Importantly, although an increase in the Ca^{2+} to Mg^{2+} ratio significantly increased cell proliferation in both normal and cancer cells, a significantly higher cell proliferation was observed in prostate cancer cells that were supplemented with higher Ca^{2+}/Mg^{2+} concentrations (increasing Ca^{2+}/Mg^{2+} ratio; Fig. 5*B*). One possibility could be that control cells could have more dying/dead cells when compared with cancer cells. Thus, we quantified live *versus* dead cells under these conditions. As shown in Fig. 5*B*, no significant change in the number of live *versus* dead cells was observed in either condition, further suggesting that increased MagNuM activity (as shown in Fig. 4) could be the reason for increased cell proliferation.

To further establish that the increase in cell proliferation was dependent on TRPM7 expression, we silenced TRPM7 in these cells. As shown in Fig. 5*C*, expression of TRPM7 siRNA in RWPE or DU145 cells led to a significant decrease in TRPM7 protein levels. Consistent with these results, a significant decrease in cell proliferation was also observed in cells expressing TRPM7 siRNA. Importantly, inhibition of TRPM7 activity by either 2APB or a decrease in the extracellular concentration of divalent cation (by adding EGTA) also inhibited cell proliferation. These results further support the data presented in previous figures that a decreased Mg^{2+} concentration along with a subsequent increase in Ca^{2+} will increase cell proliferation and thus could lead to the cancerous phenotype in prostate cells.

Higher Serum Ca^{2+}/Mg^{2+} Ratio and Increased TRPM7 Expression Were Observed in Prostate Cancer Patients—To further establish that indeed a decrease in the Ca^{2+} to Mg^{2+} ratio could lead to cancer, we next evaluated the serum Ca^{2+} and Mg^{2+} concentrations in age-matched control and prostate cancer patients. Records from medical charts of 84 patients newly diagnosed with prostate cancer and 65 patients without any cancer for whom serum Ca^{2+} and Mg^{2+} were measured were included in the analyses of prostate cancer risk. The median age (range) was 68 (52–91) years for men with prostate cancer and 72 (52–91) years for controls. Importantly, although no significant change in the corrected serum Ca^{2+} or Mg^{2+} levels was observed in prostate cancer patients, a significant increase in the Ca^{2+} to Mg^{2+} ratio was observed in prostate cancer patients (Fig. 6*A*). Overall, the results presented here suggest

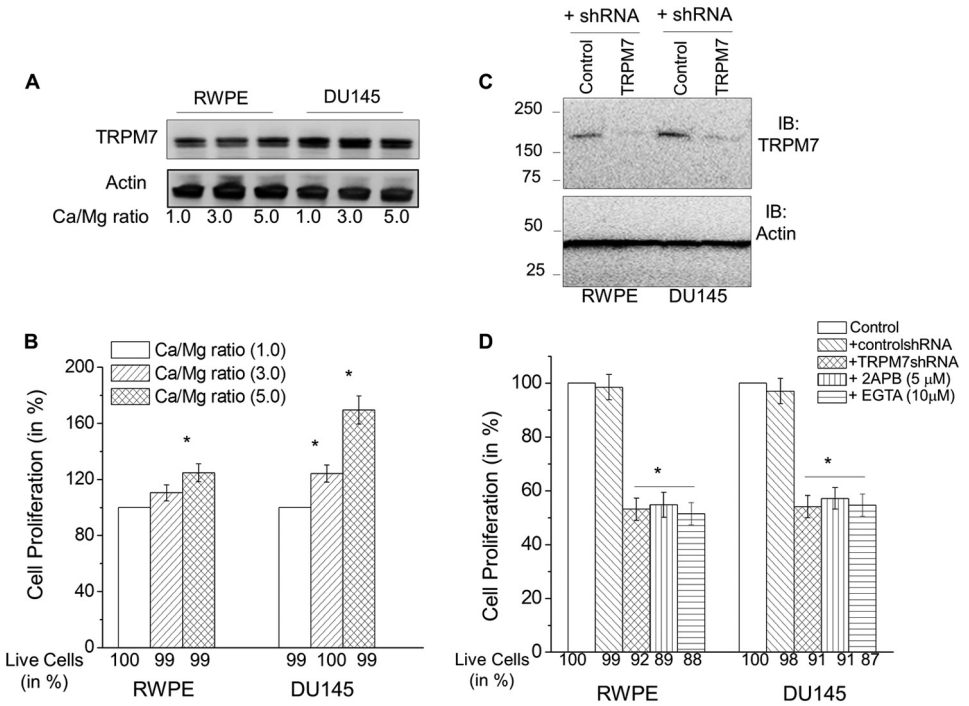

FIGURE 5. **Increased calcium entry via the MagNuM channels increased cell proliferation.** *A*, representative blots indicating the expression of TRPM7 under various Ca^{2+}/Mg^{2+} conditions. Cell lysates from control (RWPE) and DU145 cells were resolved on NuPAGE 3–8% Tris acetate gels and analyzed by Western blotting. Antibodies used are labeled in the figure; β-actin was used as a loading control. *B*, cell proliferation (MTT assays) under different Ca^{2+}/Mg^{2+} ratios in control RWPE and DU145 cells. Values are normalized and expressed as percentages. * indicates significance ($p < 0.05$) *versus* control. The number of live cells in each condition was quantified using trypan blue and is shown as a percentage at the *bottom* of the bar graph. *C*, representative Western blots indicating the expression of TRPM7 in RWPE and DU145 cells expressing either control or TRPM7 shRNA. The *top panel* was probed with TRPM7 antibodies; the *bottom panel* was probed with control actin antibodies. *D*, cell proliferation (MTT assay) under different conditions of varying Ca^{2+}/Mg^{2+} ratios in RWPE and DU145 cells. Values are expressed as percent change (mean ± S.E.). * indicates significance ($p < 0.05$) *versus* control cells. The number of live cells in each condition was quantified using trypan blue and is shown as a percentage. *IB*, immunoblot. *Error bars* represent ±S.E.

that an increase in the serum Ca^{2+} to Mg^{2+} ratio, which will increase Ca^{2+} entry by the activation of TRPM7 channels, can lead to an increase in cell proliferation and a cancer phenotype. We further assayed the expression of TRPM7 in age-matched control and prostate cancer samples. As indicated in Fig. 6*B*, a significant increase in TRPM7 expression was observed in prostate cancer samples when compared with controls. These results further suggest that increased TRPM7 expression in prostate cancer could lead to an altered Ca^{2+} to Mg^{2+} ratio, which can play a critical role in either prostate cancer initiation or its progression. More research is needed to evaluate its role in prostate cancer.

DISCUSSION

In the present study, we have characterized the functional characteristics of MagNuM currents in prostate cells. TRPM channels are widely expressed in cells including prostate tissues (34). Here we found that TRPM7 channels were expressed and functional in both normal prostate cells (RWPE) and prostate cancer cells (DU145 and PC3). Interestingly, the characteristics of the MagNuM currents observed in these cells were similar to those of TRPM7 (21, 32, 35). In addition, we also present novel evidence that currents of prostate cancer cells are more sensitive to alterations in the Ca^{2+}/Mg^{2+} ratio. Under the physiological extracellular Mg^{2+} condition, prostate cells exhibited large TRPM7-like currents that were capable of Ca^{2+} influx. Moreover, we also found that TRPM7 channel activity was dependent on intracellular Mg-ATP levels, and a decrease in intracellular Mg-ATP facilitated divalent cation entry through TRPM7 channels. Although there are conflicting reports with regard to the effect of Mg-ATP on TRPM7 channels (36), our results indicate that an increase in Mg-ATP inhibits TRPM7 currents in prostate cells. One caveat in these results is that although these cell lines are used extensively they do not truly represent the prostate cancer phenotype, and thus more research is needed to establish the role of TRPM7 in prostate cancer.

TRPM7 has been shown to be expressed in prostate cells; however, its function in these cells has not been established. Importantly, unlike TRPM6, which is expressed only in epithelial cells, TRPM7 expression is widespread. Although both TRPM6 and TRPM7 have been shown to be permeable to both Ca^{2+} and Mg^{2+} cations, our data strongly suggest that TRPM7 is essential for prostate cells. Additionally, although there is general consensus that the channel is inhibited by free intracellular Mg^{2+}, the functional roles of intracellular levels of Mg-ATP and the ability to bring in Ca^{2+} along with its physiological consequence have not yet been identified. Additionally, TRPM6 and TRPM7 channels have unique kinase domains, and although the function of the kinase domain is not fully understood (20, 21, 37), the permeability of these channels to divalent cations seems to be essential for cell viability (20, 21, 24, 31, 33, 37) and maintenance of the Mg^{2+} homeostasis in humans (23,

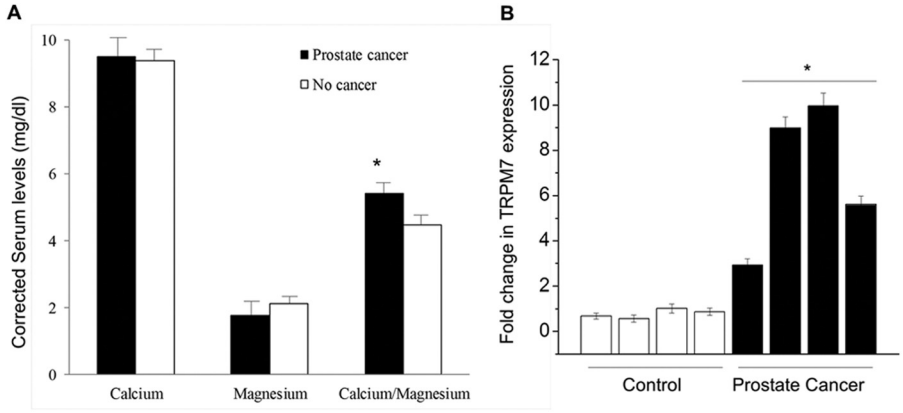

FIGURE 6. **Higher serum calcium to magnesium ratio and TRPM7 expression were observed in newly diagnosed prostate cancer patients.** *A*, serum calcium and magnesium levels (in mg/dl) were obtained from age-matched control (cases that had measured magnesium; a total of three cases) and prostate cancer patients (positive biopsies that had measured magnesium at the date of their diagnosis; a total of 25 cases). Total serum calcium was adjusted using albumin that was estimated to be at 4 g/dl by a standard formula (corrected serum calcium = total calcium + 0.8 × (4 − patients albumin)). Values are expressed as mean ± S.D. * indicates significance ($p < 0.05$). *B*, RNA was extracted from four controls and age-matched prostate cancer samples, and quantitative RT-PCR was performed. Values represent mean ± S.E. of -fold change in TRPM7 expression when compared with GAPDH from at least two independent experiments. Values are expressed as mean ± S.E.

38, 39). Functional characteristics of TRPM7 channels have been studied in several cells, but their role in cancer cells and specifically in prostate cancer is still unknown.

Mg^{2+} plays essential physiological roles as a cofactor of numerous enzymes, as a modulator of ion channels and membrane transporters, and in the regulation of cell proliferation (12, 13, 15). Mg^{2+} deficiency is also a known risk factor for predisposition to leukemias, and 46% of tertiary cancer patients present with hypomagnesia. Additionally, Mg^{2+} deficiency seems to be carcinogenic, and in the case of solid tumors, a high level of supplemented Mg^{2+} inhibits carcinogenesis (13); however, the mechanism is not known (15). One of the most important findings that we have reported here is that a decrease in intracellular Mg^{2+} concentration led to an influx of Ca^{2+}. Although both control and prostate cancer cells showed an increase in Ca^{2+} influx, the amount of Ca^{2+} influx in prostate cancer cells was higher as compared with normal cells. Consistent with these results, an increase in extracellular Ca^{2+} concentrations also led to a significant increase in cell proliferation in prostate cancer cells. In addition, a subsequent decrease in serum Mg^{2+} concentration along with an increase in Ca^{2+} concentrations to obtain a higher Ca^{2+}/Mg^{2+} ratio not only increased MagNuM currents but also increased cell proliferation. This was specifically evident in prostate cancer cells, which showed a significant increase in cell proliferation as compared with control cells. Collectively, these results suggest that alterations in the Ca^{2+}/Mg^{2+} ratio facilitate Ca^{2+} influx via the MagNuM channel and that this increase in Ca^{2+} promotes cell proliferation that can lead to cancer. These results are consistent with previous reports that have shown the relationship of MagNuM currents in regulating cell proliferation (40). Consistent with these results, an increase in the serum Ca^{2+} to Mg^{2+} ratio and TRPM7 expression was observed in prostate cancer patients, further indicating that the serum Ca^{2+} to Mg^{2+} ratio, rather than individual Ca^{2+} or Mg^{2+} concentrations in the serum, is the deciding factor leading to the increase in cell proliferation. These results are also consistent with a recent report that also showed a higher Ca^{2+}/Mg^{2+} ratio in prostate cancer patients (10); however, the mechanism was not identified in this report. Importantly, in addition, these two reports suggest that the Ca^{2+}/Mg^{2+} ratio can also be used for the diagnosis of prostate cancer. More research is needed to correlate its significance with regard to prostate-specific antigen levels and different grades of prostate cancer.

To functionally characterize the identity of the MagNuM channel, we used both pharmacological (2APB) and genetic approaches (silencing and overexpression). It has been shown previously that 2APB facilitates TRPM6-mediated magnesium currents, whereas TRPM7 inhibits the MagNuM currents. The results presented here showed an inhibition in the magnesium currents upon addition of 2APB, suggesting that TRPM7 rather than TRPM6 underlies this current. Consistent with this, silencing of TRPM7 not only decreased MagNuM currents but also inhibited cell proliferation. Conversely, increased expression of TRPM7 was also observed in prostate cancer cells when compared with control cells. This increase in TRPM7 could also account for the difference in the channel characteristics. Interestingly, no change in the expression levels of TRPM7 was observed in different Ca^{2+} to Mg^{2+} ratios, suggesting that the functional differences in MagNuM currents are not due to altered expression of TRPM7 but rather are dependent on the extracellular Ca^{2+} or Mg^{2+} levels. Overall, the results presented here suggest that in prostate cells MagNuM currents are mediated by TRPM7. Furthermore, the Ca^{2+} to Mg^{2+} ratio, which facilitates Ca^{2+} entry, was increased in cancer cells and led to an increase in cell proliferation. Thus, inhibiting TRPM7 activity (by using 2APB) can limit cell proliferation.

Acknowledgments—We acknowledge The Edward C. Carlson Imaging and Image Analysis core facility (supported in part by National Institutes of Health Grant P20RR017699) and thank Sarah Abrahamson for technical advice. We also thank Dr. Loren Runnels for providing the HA-TRPM7 construct.

REFERENCES

1. Berridge, M. J., Brown, K. D., Irvine, R. F., and Heslop, J. P. (1985) Phosphoinositides and cell proliferation. *J. Cell Sci. Suppl.* **3,** 187–198
2. Whitfield, J. F., Boynton, A. L., MacManus, J. P., Sikorska, M., and Tsang, B. K. (1979) The regulation of cell proliferation by calcium and cyclic AMP. *Mol. Cell. Biochem.* **27,** 155–179
3. Roderick, H. L., and Cook, S. J. (2008) Ca^{2+} signalling checkpoints in cancer: remodelling Ca^{2+} for cancer cell proliferation and survival. *Nat. Rev. Cancer* **8,** 361–375
4. Flourakis, M., and Prevarskaya, N. (2009) Insights into Ca^{2+} homeostasis of advanced prostate cancer cells. *Biochim. Biophys. Acta* **1793,** 1105–1109
5. Prevarskaya, N., Skryma, R., and Shuba, Y. (2004) Ca^{2+} homeostasis in apoptotic resistance of prostate cancer cells. *Biochem. Biophys. Res. Commun.* **322,** 1326–1335
6. Wissenbach, U., Niemeyer, B., Himmerkus, N., Fixemer, T., Bonkhoff, H., and Flockerzi, V. (2004) TRPV6 and prostate cancer: cancer growth beyond the prostate correlates with increased TRPV6 Ca^{2+} channel expression. *Biochem. Biophys. Res. Commun.* **322,** 1359–1363
7. Zhang, L., and Barritt, G. J. (2006) TRPM8 in prostate cancer cells: a potential diagnostic and prognostic marker with a secretory function? *Endocr. Relat. Cancer* **13,** 27–38
8. Sun, Y. H., Gao, X., Tang, Y. J., Xu, C. L., and Wang, L. H. (2006) Androgens induce increases in intracellular calcium via a G protein-coupled receptor in LNCaP prostate cancer cells. *J. Androl.* **27,** 671–678
9. Gong, Y., Blok, L. J., Perry, J. E., Lindzey, J. K., and Tindall, D. J. (1995) Calcium regulation of androgen receptor expression in the human prostate cancer cell line LNCaP. *Endocrinology* **136,** 2172–2178
10. Dai, Q., Motley, S. S., Smith, J. A., Jr., Concepcion, R., Barocas, D., Byerly, S., and Fowke, J. H. (2011) Blood magnesium, and the interaction with calcium, on the risk of high-grade prostate cancer. *PLoS One* **6,** e18237
11. Sahmoun, A. E., and Singh, B. B. (2010) Does a higher ratio of serum calcium to magnesium increase the risk for postmenopausal breast cancer? *Med. Hypotheses* **75,** 315–318
12. Hazelton, B., Mitchell, B., and Tupper, J. (1979) Calcium, magnesium, and growth control in the WI-38 human fibroblast cell. *J. Cell Biol.* **83,** 487–498
13. Anghileri, L. J. (2009) Magnesium, calcium and cancer. *Magnes. Res.* **22,** 247–255
14. Wolf, F. I., Fasanella, S., Tedesco, B., Torsello, A., Sgambato, A., Faraglia, B., Palozza, P., Boninsegna, A., and Cittadini, A. (2004) Regulation of magnesium content during proliferation of mammary epithelial cells (HC-11). *Front. Biosci.* **9,** 2056–2062
15. Rubin, H. (2005) Central roles of Mg^{2+} and $MgATP^{2-}$ in the regulation of protein synthesis and cell proliferation: significance for neoplastic transformation. *Adv. Cancer Res.* **93,** 1–58
16. Hajnóczky, G., Davies, E., and Madesh, M. (2003) Calcium signaling and apoptosis. *Biochem. Biophys. Res. Commun.* **304,** 445–454
17. Rizzuto, R., Pinton, P., Ferrari, D., Chami, M., Szabadkai, G., Magalhães, P. J., Di Virgilio, F., and Pozzan, T. (2003) Calcium and apoptosis: facts and hypotheses. *Oncogene* **22,** 8619–8627
18. Harteneck, C., Plant, T. D., and Schultz, G. (2000) From worm to man: three subfamilies of TRP channels. *Trends Neurosci.* **23,** 159–166
19. Montell, C. (2003) Mg^{2+} homeostasis: the Mg^{2+}nificent TRPM chanzymes. *Curr. Biol.* **13,** R799–R801
20. Nadler, M. J., Hermosura, M. C., Inabe, K., Perraud, A. L., Zhu, Q., Stokes, A. J., Kurosaki, T., Kinet, J. P., Penner, R., Scharenberg, A. M., and Fleig, A. (2001) LTRPC7 is a Mg·ATP-regulated divalent cation channel required for cell viability. *Nature* **411,** 590–595
21. Runnels, L. W., Yue, L., and Clapham, D. E. (2001) TRP-PLIK, a bifunctional protein with kinase and ion channel activities. *Science* **291,** 1043–1047
22. Runnels, L. W. (2011) TRPM6 and TRPM7: a Mul-TRP-PLIK-cation of channel functions. *Curr. Pharm. Biotechnol.* **12,** 42–53
23. Chubanov, V., Waldegger, S., Mederos y Schnitzler, M., Vitzthum, H., Sassen, M. C., Seyberth, H. W., Konrad, M., and Gudermann, T. (2004) Disruption of TRPM6/TRPM7 complex formation by a mutation in the *TRPM6* gene causes hypomagnesemia with secondary hypocalcemia. *Proc. Natl. Acad. Sci. U.S.A.* **101,** 2894–2899
24. Schmitz, C., Deason, F., and Perraud, A. L. (2007) Molecular components of vertebrate Mg^{2+}-homeostasis regulation. *Magnes. Res.* **20,** 6–18
25. Singh, B. B., Lockwich, T. P., Bandyopadhyay, B. C., Liu, X., Bollimuntha, S., Brazer, S. C., Combs, C., Das, S., Leenders, A. G., Sheng, Z. H., Knepper, M. A., Ambudkar, S. V., and Ambudkar, I. S. (2004) VAMP2-dependent exocytosis regulates plasma membrane insertion of TRPC3 channels and contributes to agonist-stimulated Ca^{2+} influx. *Mol. Cell* **15,** 635–646
26. Pani, B., Cornatzer, E., Cornatzer, W., Shin, D. M., Pittelkow, M. R., Hovnanian, A., Ambudkar, I. S., and Singh, B. B. (2006) Up-regulation of transient receptor potential canonical 1 (TRPC1) following sarco(endo)plasmic reticulum Ca^{2+} ATPase 2 gene silencing promotes cell survival: a potential role for TRPC1 in Darier's disease. *Mol. Biol. Cell* **17,** 4446–4458
27. Pani, B., Ong, H. L., Brazer, S. C., Liu, X., Rauser, K., Singh, B. B., and Ambudkar, I. S. (2009) Activation of TRPC1 by STIM1 in ER-PM microdomains involves release of the channel from its scaffold caveolin-1. *Proc. Natl. Acad. Sci. U.S.A.* **106,** 20087–20092
28. Selvaraj, S., Watt, J. A., and Singh, B. B. (2009) TRPC1 inhibits apoptotic cell degeneration induced by dopaminergic neurotoxin $MPTP/MPP^+$. *Cell Calcium* **46,** 209–218
29. Jiang, X., Newell, E. W., and Schlichter, L. C. (2003) Regulation of a TRPM7-like current in rat brain microglia. *J. Biol. Chem.* **278,** 42867–42876
30. Runnels, L. W., Yue, L., and Clapham, D. E. (2002) The TRPM7 channel is inactivated by PIP_2 hydrolysis. *Nat. Cell Biol.* **4,** 329–336
31. Voets, T., Nilius, B., Hoefs, S., van der Kemp, A. W., Droogmans, G., Bindels, R. J., and Hoenderop, J. G. (2004) TRPM6 forms the Mg^{2+} influx channel involved in intestinal and renal Mg^{2+} absorption. *J. Biol. Chem.* **279,** 19–25
32. Mishra, R., Rao, V., Ta, R., Shobeiri, N., and Hill, C. E. (2009) Mg^{2+}- and MgATP-inhibited and Ca^{2+}/calmodulin-sensitive TRPM7-like current in hepatoma and hepatocytes. *Am. J. Physiol. Gastrointest. Liver Physiol.* **297,** G687–G694
33. Li, M., Du, J., Jiang, J., Ratzan, W., Su, L. T., Runnels, L. W., and Yue, L. (2007) Molecular determinants of Mg^{2+} and Ca^{2+} permeability and pH sensitivity in TRPM6 and TRPM7. *J. Biol. Chem.* **282,** 25817–25830
34. Wang, H. P., Pu, X. Y., and Wang, X. H. (2007) Distribution profiles of transient receptor potential melastatin-related and vanilloid-related channels in prostatic tissue in rat. *Asian J. Androl.* **9,** 634–640
35. Thebault, S., Alexander, R. T., Tiel Groenestege, W. M., Hoenderop, J. G., and Bindels, R. J. (2009) EGF increases TRPM6 activity and surface expression. *J. Am. Soc. Nephrol.* **20,** 78–85
36. Demeuse, P., Penner, R., and Fleig, A. (2006) TRPM7 channel is regulated by magnesium nucleotides via its kinase domain. *J. Gen. Physiol.* **127,** 421–434
37. Matsushita, M., Kozak, J. A., Shimizu, Y., McLachlin, D. T., Yamaguchi, H., Wei, F. Y., Tomizawa, K., Matsui, H., Chait, B. T., Cahalan, M. D., and Nairn, A. C. (2005) Channel function is dissociated from the intrinsic kinase activity and autophosphorylation of TRPM7/ChaK1. *J. Biol. Chem.* **280,** 20793–20803
38. Dimke, H., Hoenderop, J. G., and Bindels, R. J. (2011) Molecular basis of epithelial Ca^{2+} and Mg^{2+} transport: insights from the TRP channel family. *J. Physiol.* **589,** 1535–1542
39. Alexander, R. T., Hoenderop, J. G., and Bindels, R. J. (2008) Molecular determinants of magnesium homeostasis: insights from human disease. *J. Am. Soc. Nephrol.* **19,** 1451–1458
40. Ikari, A., Okude, C., Sawada, H., Yamazaki, Y., Sugatani, J., and Miwa, M. (2008) TRPM6 expression and cell proliferation are up-regulated by phosphorylation of ERK1/2 in renal epithelial cells. *Biochem. Biophys. Res. Commun.* **369,** 1129–1133